Journal of Crystal Growth 314 (2011) 58–61

Contents lists available at ScienceDirect

Journal of Crystal Growth

journal homepage: www.elsevier.com/locate/jcrysgro

Diamond film growth on the Mo–Re alloy foil

Xiaobin Wu *, Zhiming Yu, Yilun Gong, Jian Wang, Mengkun Tian

School of Materials Science and Engineering, Central South University, Changsha 410083, China

ARTICLE INFO

Article history:
Received 23 November 2009
Received in revised form
28 September 2010
Accepted 8 October 2010
Communicated by M. Schieber
Available online 13 October 2010

Keywords:
A1. Field emission
A3. Film
B1. Diamond

ABSTRACT

Nanocrystalline diamond film was deposited on the substrate of Mo–Re alloy foil by using a hot filament chemical vapor deposition (HFCVD) method. The morphology, band structures and crystalline structure of the film were analysed by scanning electron microscopy (SEM), Raman spectroscopy and X-ray diffractometer (XRD), respectively. The results show that the thickness of the diamond film is about 300 nm after 1 h deposition. There is a 2H-Mo_2C layer between the diamond film and the Mo–Re substrate. The values of a and the ratio c/a of Mo_2C are 3.003 and 1.579 Å, respectively. This Mo_2C layer might be formed due to carbon atoms in the gas phase diffusing into the Mo–Re alloy.

1. Introduction

Diamond has been considered as a prospective material for field emission because of its low or negative electron affinities, as well as its thermal, chemical and mechanical stabilities [1–4]. Experimental results have shown that field emission from a thin sheet of molybdenum coated with diamond is greatly enhanced, as compared with that of uncoated diamond [5,6]. Molybdenum-based alloy foil is more expensive and denser than pure Mo foil, but it possesses better ductility, toughness, thermal properties and strength. Molybdenum-based alloys have attracted considerable interest for use as structural materials for applications in aerospace fields due to their high temperature strength, thermal conductivity and corrosion resistance [7,8].

Hot filament chemical vapor deposition (HFCVD) is the simplest low pressure CVD method and it gives reproducible results. Reaction conditions, such as gas composition, substrate temperature, working pressure and gas flow rate have strong influences on diamond deposition, including interface properties, morphology and quality of the diamond film. No comprehensive reports have been published on the effects of these parameters on diamond growth on Mo–Re alloy substrates. Many studies reported that the degree of diamond nucleation and adhesion of diamond films on Molybdenum substrate using the HFCVD method are related to the formation of molybdenum carbide [9].

This paper reports on nanocrystalline diamond films deposited on a foil of Mo–Re alloy for cold field electron emission. Additionally, the crystalline structure of transition phase Mo_2C has been investigated. We deposited heavily boron-doped films by hot filament chemical vapor deposition. Desirable crystal texture and low resistivity (at the level of $10^{-2}\,\Omega\,cm$) can be simultaneously obtained by optimizing the B_2H_6/CH_4 ratios.

2. Experimental details

The deposition of diamond films was carried out in a hot filament CVD reactor. The hot filament CVD system consists of a process chamber equipped with a tungsten filament and a substrate stage that were employed for activation of gas-phase reactions and for independent control of substrate temperature, respectively. Prior to diamond deposition, the substrates were pre-treated for 10 min in an ultrasonic bath in a slurry of nanodiamond powder to provide high diamond nucleation density; a gas mixture of methane and hydrogen was used as the gas reactant. The diamond film deposition was performed in a super-high steel vacuum chamber with a background pressure less than 10^{-5} Pa; details of this equipment were given in a previous work [10]. Carburized tungsten wires were heated to 2100 °C to activate the reaction gas.

Scanning electron microscopy (SEM) was carried out using a FEI Sirion200 Field emission scanning electron microscope (FESEM), with 10 kV acceleration voltage. XRD analysis was carried out using a D/max2500 diffractometer, with monochromatized Cu$K\alpha$ radiation at 10 kV and 20 mA. The Raman spectrum was measured using a LabRaman RH800 spectrometer (UK) with an argon laser source at 488 nm wavelength. The laser power was set at 20 mW.

3. Results and discussion

Fig. 1 shows the cross-section SEM images of diamond films deposited for 1 h. The thicknesses of the substrates in Fig. 1 are

* Corresponding author. Tel.: +86 731 88830335; fax: +86 731 88876692.
E-mail address: xbwu2003@163.com (X. Wu).

0022-0248/$ - see front matter © 2010 Elsevier B.V. All rights reserved.
doi:10.1016/j.jcrysgro.2010.10.008

around 6μm and the thicknesses of the films in Fig. 1 are about 300 nm. The diamond films are from layer-by-layer growth of a single grain along its external boundary. It is clearly visible in Fig. 1 that there are three layers in total including the substrate, the transition layer and diamond thin film. A columnar microstructure of the transition layer (Mo_2C) is obviously seen, which was discussed in the following sections.

Diamond films in Fig. 2 were deposited by maintaining the substrate temperature at 730 °C at6 different methane concentrations of 1% Table 1 in H_2. Fig. 2 shows the SEM morphologies of diamond films and boron-doped diamond films.

The observed grain refinement under high boron doping conditions can be explained by the increase in diamond nucleation density due to boron doping [11]. In over-doped films with very high boron concentrations only a small portion of boron atoms can replace carbon atoms and enter the texture of diamond films, while most other boron atoms accumulate at the crystal boundaries, which induces more structural defects, damages the integrity of grain and affects the electric properties of the films. Besides, more activated boron atoms in a reactive atmosphere may hinder diamond growth on the substrate and reduce the percentage of diamond phase in the films.

Fig. 3 displays the Raman spectra of the boron-doped diamond films with different boron contents . Compared to the sample without boron, intensity of the characteristic peak for diamond at 1332 cm^{-1} reduces remarkably. At the same time, new broad Raman peaks around 500 and 1220 cm^{-1} becomes noticeable when the B_2H_6/CH_4 ratio exceeds 1%, which can be related to the locally disordered structures induced by heavy boron doping [12–14].

Fig. 4 show the XRD pattern of the sample deposited with the methane concentration of 2%. One can see the peaks at $2\theta=44°$ and 75°, which correspond to diffractions from diamond (1 1 1) and (2 2 0) planes. It is also found that the peaksat $2\theta=40.40°$, 58.58°, 73.64° and 115.96° correspond to diffractions from the (1 1 0), (2 0 0), (2 1 1) and (2 2 2) planes of the Mo–Re alloy, respectively. It indicates that the Mo–Re alloy is also in a bcc structure and implies that Mo atoms are partly substituted by Re atoms. It is interesting that all of the angles from Mo–Re are less than calculated angles considering a pure bcc Mo metal with a lattice constant $a=3.147$ nm. It means that the lattice constant of the bcc Mo–Re alloy is larger than 3.147 nm. This probably implies that the radius of Re atoms in the lattice of the Mo–Re alloy is larger than 1.363 nm.

Furthermore, there are at least 15 peaks corresponds the metallic compound Mo_2C in Fig. 4. The valves of these 2θ are shown in Table 2. It indicates that molybdelum carbide is in a

Table 1
Experimental parameters for diamond deposition.

Parameters	
Filament temperature (°C)	2100–2300
Substrate temperature (°C)	730 ± 30
Spacing between filament and substrate (mm)	8
Ratio CH_4:H_2 (%)	1
Ratio B_2H_6:CH_4 (%)	1–4
Pressure (Torr)	30
Deposition time (min)	60
Total gas flow (cm^3/min)	50

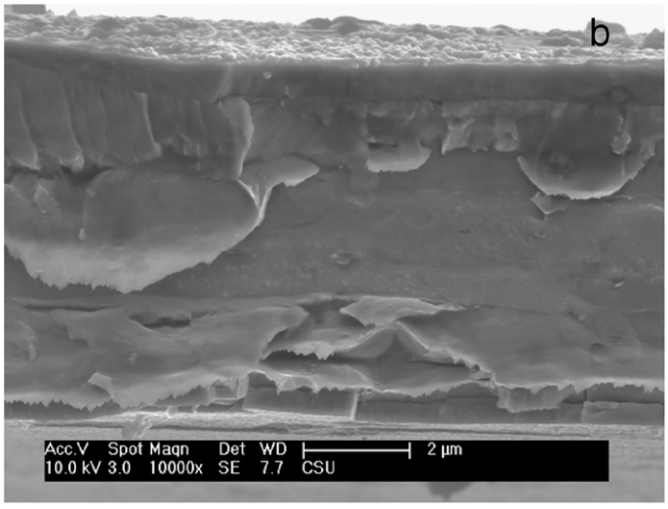

Fig. 1. SEM images of diamond films grown at methane concentrations of 1%.

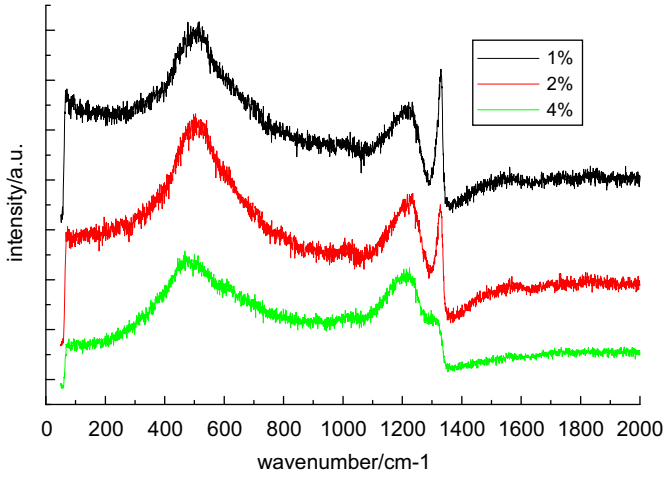

Fig. 3. Raman spectrum for boron-doped diamond films.

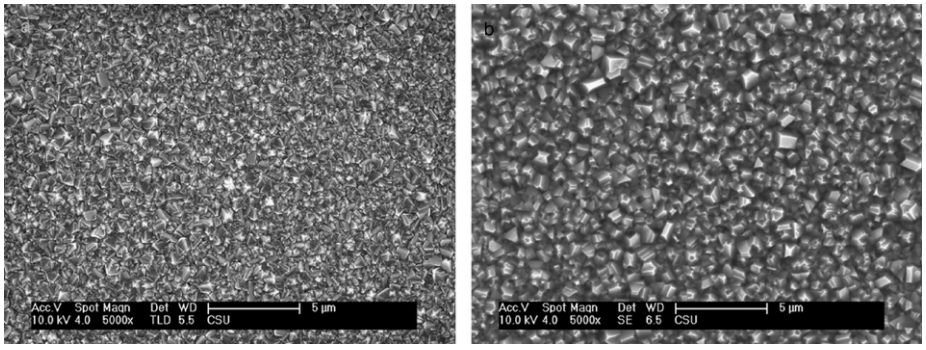

Fig. 2. SEM images of diamond films and boron-doped diamond films.

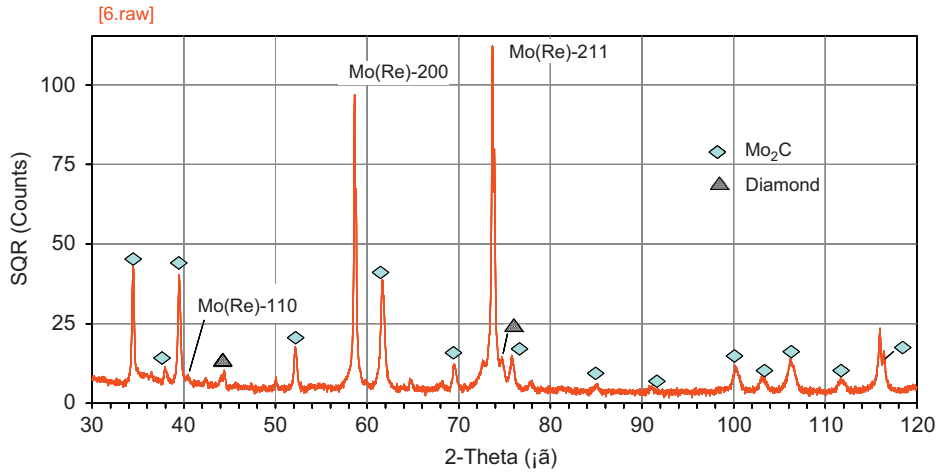

Fig. 4. XRD patterns of sample surfaces in the case of as-deposited Mo –Re foil (▲: diamond, ■: Mo_2C).

Table 2
Measured 2θ values of 2H-Mo_2C.

Planes	(1 0 0)	(0 0 2)	(1 0 1)	(1 0 2)	(1 1 0)	(0 1 3)	(2 0 0)	(1 1 2)	(2 0 1)	(2 0 2)	(0 2 3)	(2 1 0)	(2 1 1)	(1 1 4)	(2 1 2)
2θ (deg.)	34.52	37.95	39.45	52.15	61.64	69.5	72.6	74.72	75.8	85.05	100.15	103.1	106.2	111.8	116.3

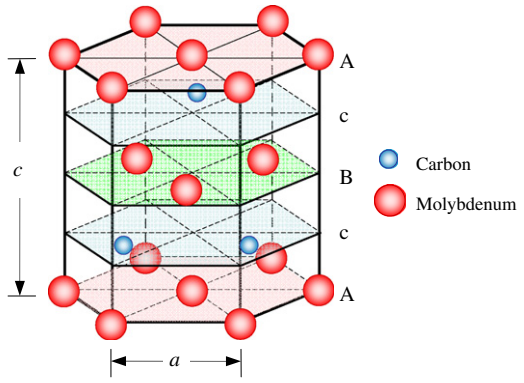

Fig. 5. Schematic representation of crystalline structure of 2H-Mo_2C.

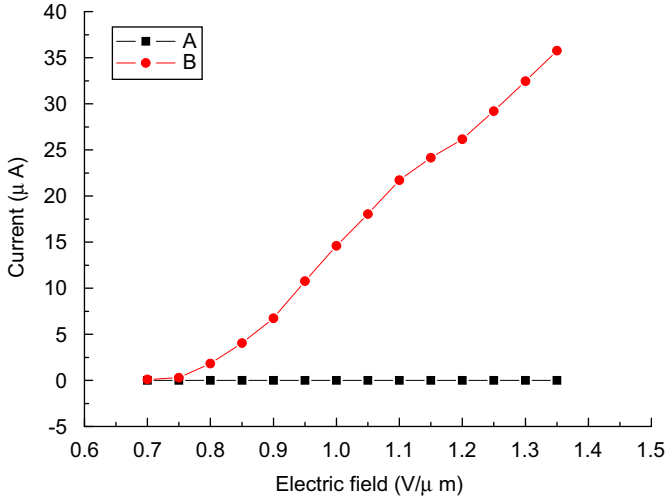

Fig. 6. Characteristics of field emission of boron-doped diamond (B) and undoped diamond (A).

hexagonal structure, i.e. 2H-Mo_2C. In the metallic compound Mo_2C, carbon atoms are inserted interstitially in half-octahedral sites of the HCP of molybdenum atoms. The crystalline structure of 2H-Mo_2C is schematically shown in Fig. 5. Its parking sequence is in principle AcBcAc etc. where A and B denote the normal sites in the HCP lattice and c denotes the interstitial site. The diffraction angle of the 2H-Mo_2C is determined by

$$\theta = \arcsin\left(\frac{\lambda}{2}\sqrt{\frac{h^2+hk+k^2}{a^2}+\frac{l^2}{c^2}}\right)$$

It is, therefore, found from the data in Table 2 that the values of a and the ratio c/a of the metallic compound are 3.003 and 1.579 Å, respectively. The measured value of the ratio c/a is less than 1.633, meaning that the carbon atoms in Mo_2C attract their nearest neighboring Mo atom. The Mo_2C formation may be due to carbon atoms in the gas phase diffusing into the Mo–Re alloy at the deposition temperature of about 730 °C.

Field emission characteristics were measured at room temperature as a function of the electric field between the sample and the anode at a vacuum of 10^{-6} Torr. Typical current (J) and voltage (V) characteristics are shown in Fig. 6.

It is clear that the boron-doped diamond-like carbon film possesses excellent field emission properties. The emission anode current (I_a) of the doped diamond film was approximately 4 μA at an electric field of 0.85 V/μm. The emission anode current of the undoped diamond film is 0 μA when the electric field does not exceed 1.4 V/μm .The modification of the FEE characteristics of diamond films can be attributed to the changes in grain size and sp2 phase concentration [15]. Electrical conductivity and/or conduction mechanism are also an important factors influencing the mission behaviour of the emitter material.

4. Conclusion

Diamond film was deposited on a Mo–Re foil substrate of thickness 6 μm through hot filament chemical vapor deposition.

It is found that the foil of the Mo–Re alloy is in a substitutional solid solution. The thickness of the the diamond film is about 300 nm after 1 h deposition. It is also found that there is a 2H-Mo_2C layer between diamond film and the Mo–Re substrate. The values of a and the ratio c/a of the metallic compound are 3.003 and 1.579 Å, respectively. This Mo_2C layer might be due to carbon atoms in the gas phase diffusing into the Mo–Re alloy at the temperature of about 730 °C. From the observed results, it is clear that the boron-doped CVD diamond films lead to improvement in their field emission characteristics.

References

[1] John C. Angus, Cliff C. Hayman, Science 241 (4868) (1988) 913–921.
[2] Kenji Hirakuri, Takahiro Yokoyama, Hirofumi Enomoto, Journal of Applied Physics 89 (2001) 8253–8258.
[3] F.J. Himpsel, J.A. Knapp, J.A. VanVechten, D.E. Eastman, Physical Review B 20 (1979) 624–627.
[4] Y.D. Kima, W. Choi, H. Wakimoto, S. Usami, H. Tomokage, T. Ando, Applied Physics Letters 75 (20) (1999) 3219–3221.
[5] Grazyna Antczak, Theodore E. Madey, Maria Blaszczyszyn, Ryszard Blaszczyszyn, Vacuum 63 (2001) 43–51.
[6] V.V. Zhimov, W.B. Choi, j.j. Cuomo, j.j. Hren, Applied Surface Science 94/95 (1996) 123–128.
[7] S.A. Fabritsiev, A.S. Pokrovsky, Journal of Nuclear Materials 252 (1998) 216–227.
[8] R.L. Mannheim, J.L. Garin, Journal of Materials Processing Technology 143–144 (2003) 533–538.
[9] Yasutaka Ando, Shogo Tobe, Hirokazu Tahara, Vacuum 83 (2009) 102–106.
[10] Z. YU, U. Karlsson, A. Flodström, Thin Solid Films 342 (1999) 74–82.
[11] X.Z. Liao, R.J. Zhang, C.S. Lee, Diamond and Related Materials 6 (1997) 521–525; X.Z. Liao, R.J. Zhang, C.S. Lee, Diamond and Related Materials 14 (2005).
[12] A.F. Azevedo, R.C. Mendes de BarrosS, H.P. Serrano, Surface and Coatings Technology 200 (2006) 5973–5977.
[13] P.C. Ricci, A. Anedda, C.M. Carbonaro, Thin Solid Films 482 (2005) 311–317.
[14] P.W. May, W.J. Ludlow, M. Hannway, P.J. Heard, J.A. Smith, K.N. Rosser, Diamond and Related Materials 17 (2008) 105–109.
[15] X. Lu, Q. Yang, C. Xiao, Thin Solid Films 516 (2008) 4217–4221.